Syntheses, X-ray Crystal Structures, and Fluxional Behavior of the Clusters $Cp^*_3Co_3(\mu_2\text{-}CO)(\mu_3\text{-}CO)(\mu\text{-}H)_2$, $Cp^*_3Co_3(\mu_2\text{-}H)(\mu_3\text{-}\eta^2\text{-}HC{=}NCMe_3)$, and $Cp^*_3Co_3(\mu_2\text{-}H)(\mu_3\text{-}\eta^2\text{-}HC{=}NCMe_2CH_2Me)$

Charles P. Casey,* Ross A. Widenhoefer, Susan L. Hallenbeck, Randy K. Hayashi, and James A. Gavney, Jr.

Department of Chemistry, University of Wisconsin, Madison, Wisconsin 53706

Received June 16, 1994[⊗]

$Cp^*_3Co_3(\mu_2\text{-}H)_3(\mu_3\text{-}H)$ (**1**) reacts with 2 equiv of CO to form the 48-electron dicarbonyl dihydride cluster $Cp^*_3Co_3(\mu_2\text{-}CO)(\mu_3\text{-}CO)(\mu\text{-}H)_2$ (**2**), which was studied by X-ray crystallography. **2** consists of an equilateral triangle of cobalt atoms (Co–Co = 2.476(1) Å) capped on each face by a μ-CO ligand. Line-shape analysis of the CO region in the variable temperature ^{13}C NMR of **2** allowed the barrier for interconversion of the μ_2- and μ_3-CO ligands to be measured ($\Delta G^{\ddagger}$ = 8.6(1) kcal mol^{-1}). Cluster **2** loses H_2 at 80 °C ($\Delta G^{\ddagger}$ = 26(1) kcal mol^{-1}) to form the 46-electron dicarbonyl cluster $Cp^*_3Co_3(\mu_3\text{-}CO)_2$ (**3**). **3** reacts with 5.4 atm of H_2 at 80 °C to form a 1.1:1 equilibrium mixture of **2** and **3** (ΔG = −2.6(1) kcal mol^{-1}). *tert*-Butyl isocyanide reacts with **1** at −35 °C to form the bis(isocyanide) cluster $Cp^*_3Co_3(\mu\text{-}CNCMe_3)_2(\mu\text{-}H)_2$ (**10**), which was observed by low-temperature ^1H NMR spectroscopy. A coordinated *tert*-butyl isocyanide ligand rapidly inserted into a cobalt–hydrogen bond of **10** to produce the formimidoyl cluster $Cp^*_3Co_3(\mu_2\text{-}H)(\mu_3\text{-}\eta^2\text{-}CH{=}NCMe_3)$ (**4**). Likewise, the reaction of *tert*-amyl isocyanide with **1** formed $Cp^*_3Co_3(\mu_2\text{-}H)(\mu_3\text{-}\eta^2\text{-}CH{=}NCMe_2CH_2Me)$ (**11**). Clusters **4** and **11** were characterized by X-ray crystallography and were shown to consist of a triangle of cobalt atoms capped on one face by a $\mu_3\text{-}\eta^2$-formimidoyl ligand and capped on the opposite face by a μ-hydride ligand. Line shape analysis of the Cp* region in the variable temperature ^1H NMR of cluster **4** allowed the barrier for complete rotation of the formimidoyl ligand parallel to the tricobalt plane to be measured ($\Delta G^{\ddagger}$ = 9.9(1) kcal mol^{-1}).

Introduction

We have been exploring the reactions of the unusual trinuclear tetrahydride cluster $Cp^*_3Co_3(\mu_2\text{-}H)_3(\mu_3\text{-}H)$ (**1**)[1] with small unsaturated molecules in an effort to form new tricobalt derivatives. For example, we have shown that **1** reacts rapidly with NO at room temperature to form the bicapped nitrosyl cluster $Cp^*_3Co_3(\mu_3\text{-}NO)_2$.[2] Cluster **1** also reacts with acetylene to form the mono(ethylidyne) clusters $Cp^*_3Co_3(\mu_3\text{-}CCH_3)(\mu_3\text{-}H)$ and $Cp^*_3Co_3(\mu_3\text{-}CCH_3)(\mu_2\text{-}H)_3$; these mono(ethylidyne) clusters react further with acetylene to ultimately form the bis(ethylidyne) cluster $Cp^*_3Co_3(\mu_3\text{-}CCH_3)_2$ (Scheme 1).[3]

We initially showed that **1** reacted rapidly with excess CO at room temperature to fragment the cluster and form mononuclear $Cp^*Co(CO)_2$ and H_2.[1] Because there are several examples of cyclopentadienyl trimetallic clusters which possess two[4–6] or three[7] bridging CO ligands, we searched for tricobalt intermediates in the reaction of **1** and CO. Here we report that **1** reacts with 2 equiv of CO at room temperature to form the dicarbonyl dihydride cluster $Cp^*_3Co_3(\mu_3\text{-}CO)(\mu_2\text{-}CO)(\mu\text{-}H)_2$ (**2**). We have also found that **1** reacts with *tert*-butyl isocyanide at low temperature to form the bis(isocyanide) dihydride cluster $Cp^*_3Co_3(\mu\text{-}CNCMe_3)_2(\mu\text{-}H)_2$ (**10**), which is isoelectronic with the dicarbonyl dihydride cluster **2**. An isocyanide ligand of cluster **10** undergoes an unusually facile insertion into a cobalt–hydrogen bond to form the 48-electron formimidoyl cluster $Cp^*_3Co_3(\mu_2\text{-}H)(\mu_3\text{-}\eta^2\text{-}HC{=}NCMe_3)$ (**4**).[8]

Results and Discussion

Synthesis of $Cp^*_3Co_3(\mu_3\text{-}CO)(\mu_2\text{-}CO)(\mu\text{-}H)_2$ (2). When 2 equiv of CO was added to a flask containing a black benzene solution of **1**, a brown solution formed rapidly. Evaporation of solvent and crystallization from pentane gave the 48-electron dicarbonyl dihydride cluster $Cp^*_3Co_3(\mu_3\text{-}CO)(\mu_2\text{-}CO)(\mu\text{-}H)_2$ (**2**) in 60% yield (Scheme 2). Cluster **2** was characterized by spectroscopy. The ^1H NMR spectrum of **2** in benzene-d_6 displayed a 2:1 ratio of Cp* peaks and a low-frequency resonance at δ −32.26 assigned to two bridging[9] hydride

[⊗] Abstract published in *Advance ACS Abstracts,* October 15, 1994.

(1) Kersten, J. L.; Rheingold, A. L.; Theopold, K. H.; Casey, C. P.; Widenhoefer, R. A.; Hop, C. E. C. A. *Angew. Chem.* **1992**, *104*, 1364; *Angew. Chem., Int. Ed. Engl.* **1992**, *31*, 1341.

(2) Casey, C. P.; Widenhoefer, R. A.; Hayashi, R. K. *Inorg. Chim. Acta* **1993**, *212*, 81.

(3) Casey, C. P.; Widenhoefer, R. A.; Hallenbeck, S. L. *Organometallics* **1993**, *12*, 3788.

(4) Olson, W. L.; Stacy, A. M.; Dahl, L. F. *J. Am. Chem. Soc.* **1986**, *108*, 7646.

(5) Bray, A. C.; Green, M.; Hankey, D. R.; Howard, J. A. K.; Johnson, O.; Stone, F. G. A. *J. Organomet. Chem.* **1985**, *281*, C12.

(6) Barnes, C. E.; Orvis, J. A.; Staley, D. L.; Rheingold, A. L.; Johnson, D. C. *J. Am. Chem. Soc.* **1989**, *111*, 4992 and references therein.

(7) (a) King, R. B. *Inorg. Chem.* **1966**, *5*, 2227. (b) Mills, O. S.; Paulus, E. F. *J. Organomet. Chem.* **1967**, *10*, 331. (c) Paulus, E. F. *Acta Crystallogr., Sect. B* **1969**, *25*, 2206. (d) Vollhardt, K. P. C.; Bercaw, J. E.; Bergman, R. G. *J. Organomet. Chem.* **1975**, *97*, 283. (e) Bailey, W. I.; Cotton, F. A.; Jamerson, J. D.; Kolthammer, B. W. S. *Inorg. Chem.* **1982**, *21*, 3131.

(8) Casey, C. P.; Widenhoefer, R. A.; Hallenbeck, S. L.; Gavney, J. A. *J. Chem. Soc., Chem. Commun.* **1993**, 1692.

0276-7333/94/2313-4720$04.50/0

Scheme 1

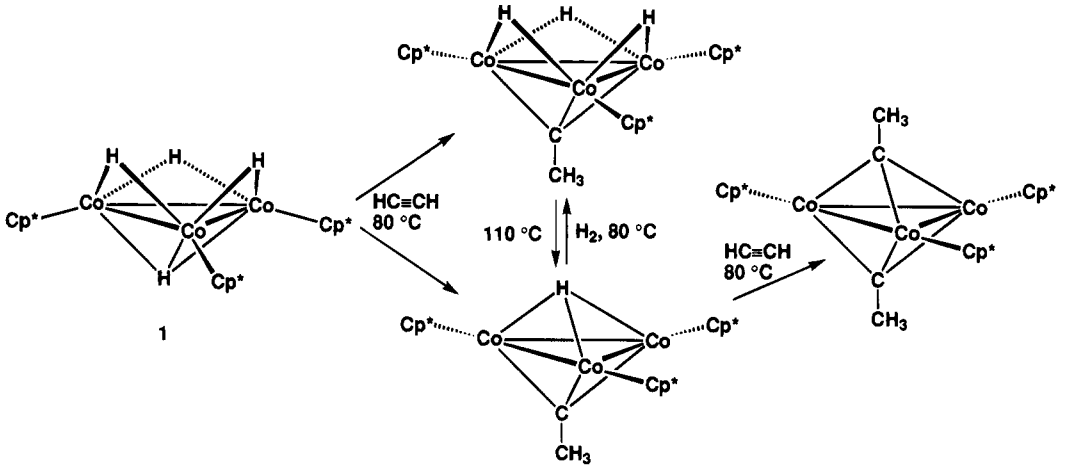

Scheme 2

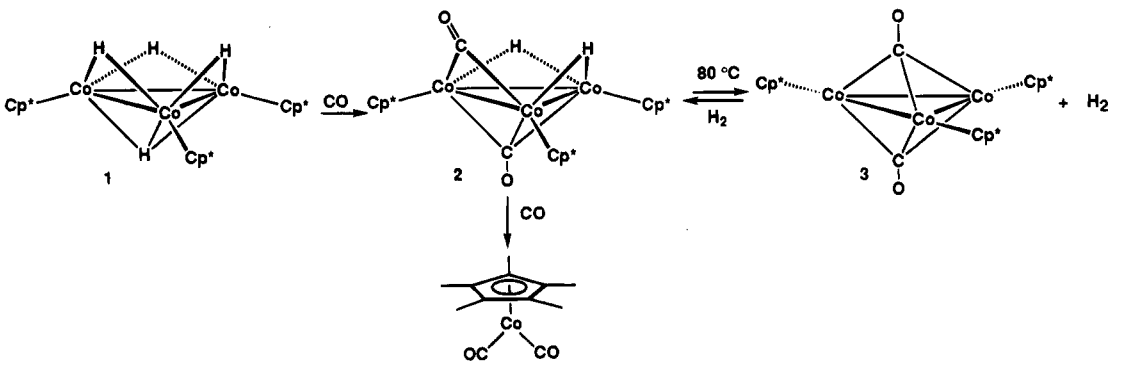

ligands. In both the solid-state and hexane solution IR spectra of **2**, intense absorbances near 1770 and 1650 cm^{-1} indicated the presence of both doubly and triply bridging CO ligands. The structure and spectroscopic properties of **2** are very similar to those of the clusters $Cp^*_3Rh_2M(\mu_3\text{-}CO)(\mu_2\text{-}CO)(\mu\text{-}H)_2$ (M = Co, Ir, Rh) reported by Stone.[5]

When a benzene-d_6 solution of **1** was progressively exposed to small amounts of CO (<1 equiv) and monitored after each addition by ^1H NMR spectroscopy, only Cp* signals for **1** (δ 62) and **2** (δ 1.56 and 1.63) were observed. The Cp* signal for $Cp^*Co(CO)_2$ at δ 1.59 was observed only after complete conversion of **1** to **2**. Isolated **2** was quantitatively (96 ± 5% by ^1H NMR) converted to $Cp^*Co(CO)_2$ upon exposure to 1 atm of CO at room temperature for 1 h. These experiments demonstrate that CO reacts much faster with the 46-electron cluster **1** than with the 48-electron cluster **2** and that **2** is an intermediate in the formation of $Cp^*Co(CO)_2$.

X-ray Crystallography of $Cp^*_3Co_3(\mu_2\text{-}CO)(\mu_3\text{-}CO)(\mu\text{-}H)_2$ (2). An X-ray crystallographic study of **2** showed that the compound crystallized in the $P6_3/m$ space group, which has both 3-fold and mirror plane symmetry not possessed by **2** in either the solid state, as shown by IR spectroscopy, or solution, as shown by both IR and NMR spectroscopy. The structure of **2** consists of an equilateral triangle of three cobalt atoms capped on each face by a μ-CO ligand (Figure 1, Tables 1 and 2). The anisotropic thermal parameters of the μ-CO ligands

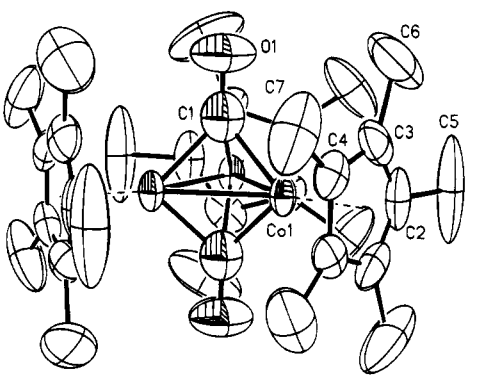

Figure 1. X-ray crystal structure for $Cp^*_3Co_3(\mu_2\text{-}CO)(\mu_3\text{-}CO)(\mu\text{-}H)_2$ (**2**) with thermal ellipsoids shown at the 35% probability level.

were large, indicative of a disordered structure. We propose that the μ_3-CO ligand occupies one cluster face while the μ_2-CO ligand and the two bridging hydride ligands occupy the opposite face. The very high crystallographic site symmetry ($3/m$) is consistent with the disorder of the bridging ligands through the mirror plane and the 3-fold axis. As a result of the disorder, no reliable information about the positions of the bridging hydride and carbonyl ligands in **2** could be obtained. The artificially high site symmetry of **2** is somewhat surprising in comparison with the isoelectronic trirhodium cluster $Cp^*_3Rh_3(\mu_2\text{-}CO)(\mu_3\text{-}CO)(\mu\text{-}H)_2$, which displayed no crystallographically imposed symmetry. However, both the mirror and 3-fold disorder of bridging ligands in $(Cp^*Co)_3$ clusters has been previously observed.[9,10]

(9) Casey, C. P.; Widenhoefer, R. A.; Hallenbeck, S. L.; Hayashi, R. K. *Inorg. Chem.* **1994**, *33*, 2639 and references therein.

Table 1. X-ray Crystal Structure Data for $Cp^*_3Co_3(\mu_2\text{-}CO)(\mu_3\text{-}CO)(\mu\text{-}H)_2$ (2), $Cp^*_3Co_3(\mu_2\text{-}H)(\mu_3\text{-}\eta^2\text{-}HC{=}NCMe_3)$ (4), and $Cp^*_3Co_3(\mu_2\text{-}H)(\mu_3\text{-}\eta^2\text{-}CH{=}NCMe_2CH_2Me)$ (11)

	2	4	11
empirical formula	$C_{32}H_{47}Co_3O_2$	$C_{35}H_{56}Co_3N$	$C_{36}H_{58}Co_3N$
color; habit	black plate	brown prisms	purple block
cryst syst	hexagonal	monoclinic	triclinic
space group	$P6_3/m$	$P2_1/n$	$P\bar{1}$
unit cell dimens			
a, Å	10.692(2)	10.580(2)	10.6943(10)
b, Å		17.340(3)	17.838(2)
c, Å	15.329(3)	17.741(4)	19.630(3)
α, deg			111.183(10)
β, deg		95.78(3)	101.039(8)
γ, deg			93.823(9)
V, Å^3	1517.6(5)	3238.2(11)	3389.2(9)
no. of peaks to determine cell	25	25	40
2θ range of cell peaks, deg	25–30	25.25–28.64	9.0–25
Z	2	4	4
fw	640.5	667.6	681.6
density (calcd), g cm^{-3}	1.402	1.369	1.336
abs coeff, mm^{-1}	1.644	1.540	1.473
$F(000)$	672	1416	1448
$R(F)$, %	5.14	6.63	6.84
$R_w(F)$, %	6.84	3.66	5.00

Table 2. Selected Bond Lengths (Å) and Angles (deg) for $Cp^*_3Co_3(\mu_3\text{-}CO)(\mu_2\text{-}CO)(\mu\text{-}H)_2$ (2)

Co(1)–Co(1a)	2.449(1)	Co(1)–C(2)	2.101(10)
Co(1)–C(1)	1.940(13)	Co(1)–C(3)	2.104(6)
C(1)–O(1)	1.199(23)	Co(1)–C(4)	2.092(5)
Co(1)–C(1)–O(1)	133.2(4)	Co(1)–Co(1a)–C(1)	50.9(3)
Co(1)–C(1)–Co(1a)	78.3(6)	C(1)–Co(1)–C(1a)	86.4(8)

The nominal Co–Co distance in the 48-electron cluster **2** (2.446 (1) Å) is somewhat longer than the Co–Co distances observed for bicapped 48-electron $Cp^*_3Co_3$ clusters, which range from 2.408 Å in $Cp^*_3Co_3(\mu_3\text{-}CCH_3)(\mu_3\text{-}NO)$[9] to 2.437 Å in $Cp^*_3Co_3(\mu_3\text{-}CMe)_2$,[10] and is considerably longer than the Co–Co distance in the 46-electron clusters $Cp^*_3Co_3(\mu_3\text{-}CO)_2$ (2.370 Å)[4] and $Cp^*_3Co_3(\mu_3\text{-}CCH_3)(\mu_3\text{-}H)$ (2.378 Å).[10] The unusually long Co–Co distance in **2** relative to those in other 48-electron $(Cp^*Co)_3$ clusters is consistent with the presence of bridging hydride ligands, which typically lengthen M–M bonds.[11]

Dehydrogenation of $Cp^*_3Co_3(\mu_2\text{-}CO)(\mu_3\text{-}CO)(\mu\text{-}H)_2$ (2). When a benzene-d_6 solution of **2** was heated at 80 °C under a nitrogen atmosphere, the known,[4] 46-electron dicarbonyl cluster $Cp^*_3Co_3(\mu_3\text{-}CO)_2$ (**3**) was formed quantitatively (99 ± 5% by ^{1}H NMR analysis). Cluster **3** was characterized on the basis of its unusual ^{1}H NMR spectrum (C_6D_6, δ 3.39) and IR spectrum (hexane, ν_{CO} 1681 cm^{-1}). The conversion of **2** to **3** at 80 °C was monitored by ^{1}H NMR spectroscopy and followed first-order kinetics for the disappearance of **2** to over 3 half-lives ($t_{1/2}$ = 28 min, $k = (4.2 \pm 0.2) \times 10^{-4}$ s^{-1}; $\Delta G^{\ddagger}$ = 26.2(1) kcal mol^{-1} at 80 ± 0.5 °C). The rate constant for H_2 loss from **2** was also measured at 60 °C ($k = (4.76 \pm 0.2) \times 10^{-5}$ s^{-1}) and 71 °C ($k = (1.54 \pm 0.05) \times 10^{-4}$ s^{-1}). An Eyring plot of the data provided the activation parameters $\Delta H^{\ddagger}$ = 24.7(4) kcal mol^{-1} and $\Delta S^{\ddagger}$ = −5(1) eu.

The dehydrogenation of **2** to **3** is reversible. When **3** was heated to 83 °C in a sealed tube under 5.4 atm of H_2 for 2 days, a 1.1:1.0 equilibrium mixture of **2**:**3** (K_{eq} = [H_2][**3**]/[**2**] = 9.2 × 10^{-3} M) was formed, as determined by ^{1}H NMR spectroscopy. The equilibrium constant was also measured at 62 °C ($K_{eq} = 1.5 \times 10^{-2}$ M) and 73 °C ($K_{eq} = 2.4 \times 10^{-2}$ M), which allowed calculation of thermodynamic parameters: ΔG° = 2.7 kcal mol^{-1}, ΔH° = 10.3 kcal mol^{-1}, and ΔS° = 21 eu at 83 ± 0.5 °C.

$$\underset{\mathbf{2}}{Cp^*_3Co_3(\mu_3\text{-}CO)(\mu_2\text{-}CO)(\mu\text{-}H)_2} \overset{K_{eq}}{\rightleftharpoons} \underset{\mathbf{3}}{Cp^*_3Co_3(\mu_3\text{-}CO)_2} + H_2$$

The reversible addition of H_2 to a metal cluster such as **2** is interesting in relation to the reversible chemisorption of H_2 on a metal surface. The reversible addition of H_2 to the unsaturated 46-electron cluster **2** is unusual, since it does not involve simultaneous loss of a ligand. The reversible addition of H_2 to a polynuclear metal complex is usually complicated by simultaneous dissociation or hydrogenation of an ancillary ligand.[12] We are aware of only four examples of the reversible addition of H_2 to metal clusters without ligand loss. Stone reported that the 46-electron mixed-metal clusters $Cp^*_3Rh_2M(\mu_3\text{-}CO)_2$ (M = Ir, Rh) add H_2 to form the 48-electron dihydride clusters $Cp^*_3Rh_2M(\mu_3\text{-}CO)(\mu_2\text{-}CO)(\mu_2\text{-}H)_2$ (M = Ir, Rh) without ligand loss.[5] The tetranuclear dihydride cluster $Os_3Pt(\mu\text{-}H)_2(CO)_{10}[P(C_6H_{11})_3]$ formed $Os_3Pt(\mu\text{-}H)_4(CO)_{10}[P(C_6H_{11})_3]$ under 200 atm of H_2 and was regenerated under an N_2 purge.[13] The 48-electron triruthenium dihydride cluster $Ru_3(CO)_8(\mu\text{-}H)_2(\mu\text{-}t\text{-}Bu_2P)_2$ reacted reversibly with H_2 via cleavage of a Ru–Ru bond to form the 50-electron cluster $Ru_3(CO)_8(\mu\text{-}H)_2(H)_2(\mu\text{-}t\text{-}Bu_2P)_2$.[14] We observed reversible H_2 addition to the 46-electron mono(ethylidyne) monohydride cluster $Cp^*_3Co_3(\mu_3\text{-}H)(\mu_3\text{-}CCH_3)$ to form the mono(ethylidyne) trihydride cluster $Cp^*_3Co_3(\mu_2\text{-}H)_3(\mu_3\text{-}CCH_3)$.[3]

Fluxionality of 2-($^{13}CO)_2$ Observed by ^{13}C NMR Spectroscopy. The presence of both doubly and triply bridging CO ligands in **2** was initially established by solution and solid-state IR spectroscopy. The ^{13}C NMR spectrum of $Cp^*_3Co_3(\mu_2\text{-}^{13}CO)(\mu_3\text{-}^{13}CO)(\mu\text{-}H)_2$ (**2**-($^{13}CO)_2$) at −90 °C in toluene-d_8 displayed a 1:1 ratio of CO resonances at δ 261 and 284 (^{59}Co quadrupole broadened, $w_{1/2}$ = 45 Hz), confirming the presence of two different types of bridging CO ligands. As the temperature was raised, the peaks broadened and coalesced at −59 °C, forming a single resonance at δ 270.9 ($w_{1/2}$ =

(10) Casey, C. P.; Widenhoefer, R. A.; Hallenbeck, S. L.; Hayashi, R. K.; Powell, D. R.; Smith, G. W. *Organometallics* **1994**, *13*, 1521.

(11) Collman, J. P.; Hegedus, L. S.; Norton, J. R.; Finke, R. G. *Principles and Applications of Organotransition Metal Chemistry*, 2nd ed.; University Science Books: Mill Valley, CA, 1987; p 83.

(12) (a) Vites, J.; Fehlner, T. P. *Organometallics* **1984**, *3*, 491. (b) Knox, S. A. R. *Pure Appl. Chem.* **1984**, *56*, 81. (c) Hill, R. H.; Puddephatt, R. J. *J. Am. Chem. Soc.* **1983**, *105*, 5797. (d) Andrews, M. A.; Kaesz, H. D. *J. Am. Chem. Soc.* **1979**, *101*, 7255. (e) Keister, J. B.; Payne, M. W.; Muscatella, M. J. *Organometallics* **1983**, *2*, 219. (f) Bavaro, L. M.; Montangero, P.; Keister, J. B. *J. Am. Chem. Soc.* **1983**, *105*, 4977. (g) Dutta, T. K.; Vites, J. C.; Fehlner, T. P. *Organometallics* **1986**, *5*, 385. (h) Roberts, D. A.; Steinmetz, G. R.; Breen, M. J.; Shulman, P. M.; Morrison, E. D.; Duttera, M. R.; DeBrosse, C. W.; Whittle, R. R.; Geoffroy, G. L. *Organometallics* **1983**, *2*, 846. (i) Breen, M. J.; Shulman, P. M.; Geoffroy, G. L.; Rheingold, A. L.; Fultz, W. C. *Organometallics* **1984**, *3*, 782. (j) Lugan, N.; Lavigne, G.; Bonnet, J.-J.; Réau, R.; Neibecker, D.; Tkatchenko, I. *J. Am. Chem. Soc.* **1988**, *110*, 5369.

(13) Farrugia, L. J.; Green, M.; Hankey, D. R.; Orpen, A. G.; Stone, F. G. A. *J. Chem. Soc., Chem. Commun.* **1983**, *310*.

(14) Arif, A. M.; Bright, T. A.; Jones, R. A.; Nunn, C. M. *J. Am. Chem. Soc.* **1988**, *110*, 6894.

Scheme 3

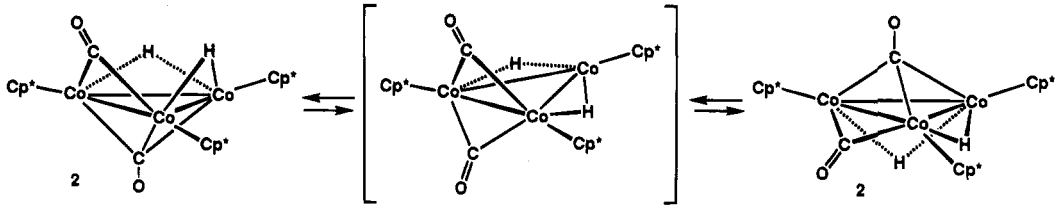

Scheme 4

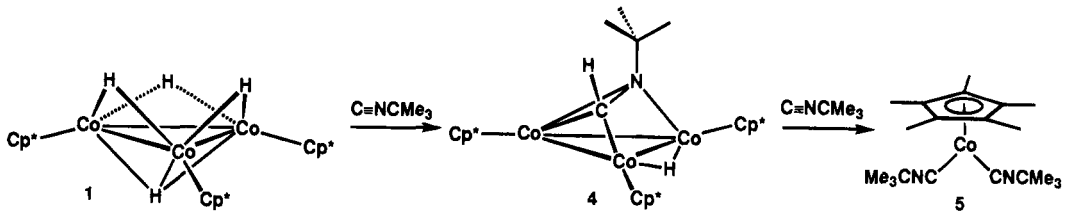

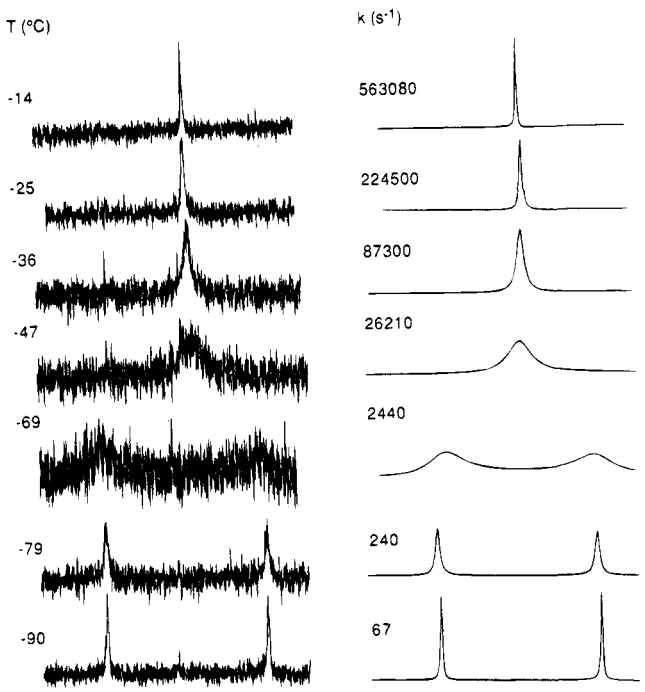

Figure 2. Variable temperature ^{13}C NMR spectra (126 MHz) of the CO region of **2**-(^{13}**CO**)$_2$. Observed spectra and temperatures are on the left. Simulated spectra and rates are on the right.

30 Hz) at −14 °C, which sharpened further ($w_{1/2}$ = 20 Hz) upon warming to room temperature. The ^1H NMR spectrum of **2** both at −90 °C and at room temperature showed a 2:1 ratio of Cp* resonances, indicating that the fluxional process that interconverts the bridging carbonyls does not interchange the Cp* ligands.

The variable temperature ^{13}C NMR spectra of the cluster **2**-(^{13}**CO**)$_2$ is consistent with the interconversion of μ_2-CO and μ_3-CO ligands about a single cluster edge (Scheme 3). Presumably, the hydride ligands also oscillate above and below the tricobalt plane in order to remain on the same face as the μ_2-CO ligand. This process creates a time-averaged symmetry plane through the three cobalt atoms which exchanges the environments of the two CO ligands but preserves the 2:1 ratio of Cp* resonances observed in the ^1H NMR spectrum. A possible intermediate in this process would be a cluster with two μ_2-CO ligands. A barrier for the interconversion of the CO ligands of $\Delta G^{\ddagger}$ = 8.6(1) kcal mol^{-1} was determined from the complete line-shape analysis of the CO resonances over the temperature range −90 to −14 °C (Figure 2). A T_2* value of 0.017 s (corresponding to $w_{1/2}$ = 20 Hz), which takes into account quadrupolar broadening by ^{59}Co, was used in the line-shape analysis. This barrier is approximately 2−3 kcal mol^{-1} less than the barrier normally seen for migration of a hydride ligand between adjacent pairs of metal atoms.[9,15]

Formimidoyl Formation from 1 and *tert*-Butyl Isocyanide. When a black solution of tricobalt tetrahydride cluster **1** was stirred with 2.5 equiv of C≡NCMe$_3$ in benzene at room temperature for 12 h, the solution turned brown. Evaporation of solvent and crystallization from pentane gave the diamagnetic formimidoyl cluster Cp*$_3$Co$_3$(μ_2-H)(μ_3-η^2-HC=NCMe$_3$) (**4**) in 52% yield (Scheme 4). The structure of **4** was determined by spectroscopy and by single-crystal X-ray diffraction. In the ^1H NMR spectrum at room temperature, resonances were observed for three averaged Cp* ligands at δ 1.86 and for a *tert*-butyl group at δ 1.53. A characteristic resonance for the formimidoyl hydrogen was observed at δ 8.69 which indicated that isocyanide insertion into a Co−H bond had occurred; a resonance of equal intensity at δ −20.42 was assigned to the single bridging hydride ligand.

Formimidoyl Cluster Breakup upon Treatment with Excess *tert*-Butyl Isocyanide. When a benzene solution of **1** and excess *tert*-butyl isocyanide (>10 equiv) was heated to 55 °C for 2.5 h, the color changed from black to orange. Evaporation of solvent and distillation of the residue gave the bis(isocyanide) monomer Cp*Co(CNCMe$_3$)$_2$ (**5**) in 45% yield as a viscous red oil (Scheme 4). ^1H NMR analysis of the reaction in benzene-d_6 with SiMe$_4$ as an internal standard showed quantitative (98 ± 5%) formation of **5**. In the ^1H NMR spectrum, resonances at δ 2.00 and 1.17 confirmed the 1:2 ratio of Cp*Co units to *tert*-butyl groups, and two intense absorbances in the IR spectrum at 2001 and 1902 cm^{-1} indicated the presence of terminal isocyanide ligands.[16]

In a separate experiment, the reaction of **1** and *tert*-butyl isocyanide (2 equiv) in C$_6$D$_6$ at room temperature

(15) (a) Keister, J. B.; Shapley, J. R. *Inorg. Chem.* **1982**, *21*, 3304. (b) Churchill, M. R.; Janik, T. S.; Duggan, T. P.; Keister, J. B. *Organometallics* **1987**, *6*, 799. (c) Nevinger, L. R.; Keister, J. B. *Organometallics* **1990**, *9*, 2312. (d) Shapley, J. R.; Richter, S. I.; Churchill, M. R.; Lashewycz, R. A. *J. Am. Chem. Soc.* **1977**, *99*, 7384.

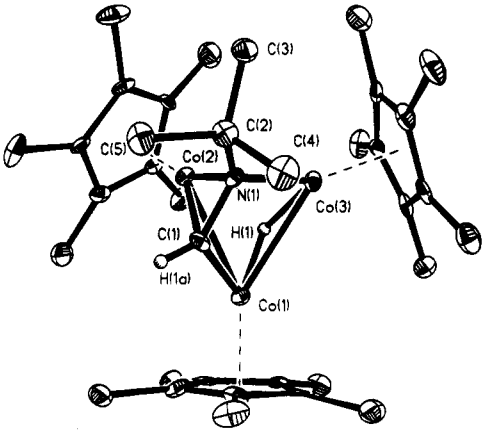

Figure 3. X-ray crystal structure of $Cp^*_3Co_3(\mu_2\text{-}H)(\mu_3\text{-}\eta^2\text{-}CH{=}NCMe_3)$ (**4**) with thermal ellipsoids shown at the 35% probability level.

Table 3. Selected Bond Lengths (Å) and Angles (deg) for $Cp^*_3Co_3(\mu_2\text{-}H)(\mu_3\text{-}\eta^2\text{-}CH{=}NCMe_3)$ (4)

Co(1)–Co(2)	2.557(1)	Co(3)–H(1)	1.653(51)
Co(1)–Co(3)	2.621(1)	C(1)–N(1)	1.346(7)
Co(2)–Co(3)	2.525(1)	C(1)–H(1a)	1.001(52)
Co(1)–C(1)	1.842(6)	C(2)–N(1)	1.509(7)
Co(2)–C(1)	1.968(5)	Co(1)–Cp_{cent}	1.756
Co(2)–N(1)	1.972(4)	Co(2)–Cp_{cent}	1.734
Co(3)–N(1)	1.912(4)	Co(3)–Cp_{cent}	1.762
Co(2)–H(1)	2.010(54)		

Co(1)–Co(2)–Co(3)	62.1(1)	Co(1)–H(1)–Co(3)	117.4(33)
Co(1)–Co(3)–Co(2)	59.6(1)	C(1)–Co(2)–N(1)	40.0(2)
Co(2)–Co(1)–Co(3)	58.3(1)	Co(1)–C(1)–N(1)	115.1(4)
Co(1)–C(1)–Co(2)	84.2(2)	Co(3)–N(1)–C(1)	104.7(3)
Co(2)–N(1)–Co(3)	81.1(2)	Co(2)–N(1)–C(2)	133.5(3)
C(1)–N(1)–C(2)	120.7(4)	Co(3)–N(1)–C(2)	129.1(3)
H(1a)–C(1)–N(1)	121.6(33)		

was analyzed by ^1H NMR spectroscopy using C_6Me_6 as an internal standard. After 1 h, the *tert*-butyl isocyanide resonance was no longer detectable, the Cp* resonance of **1** (δ 62) accounted for 8% of the Cp* resonances, and product Cp* resonances for **4** (δ 1.88) and **5** (δ 2.00) were observed in a 5:1 ratio.

Cluster **4** reacted with excess *tert*-butyl isocyanide in C_6D_6 at room temperature to generate monomer **5** quantitatively (98 ± 5% by ^1H NMR). Since no H_2, imine $H_2C{=}NCMe_3$, or imine trimer $[CH_2N(CMe_3)]_3$ was observed in this reaction, the fate of the formimidoyl ligand remains unknown.

X-ray Crystal Structure of $Cp^*_3Co_3(\mu_2\text{-}H)(\mu_3\text{-}\eta^2\text{-}HC{=}NCMe_3)$ (4). The structure of cluster **4**, determined by X-ray crystallography, consists of a triangle of cobalt atoms capped on one face by an η^2-formimidoyl ligand bonded to all three cobalt atoms (Figure 3, Tables 1 and 3). Co(1) is bonded to only C(1), Co(3) is bonded to only N(1), and Co(2) is bonded to both C(1) and N(1). The C(1)=N(1) bond is roughly parallel to both the Co(1)–Co(3) edge and the tricobalt plane. The Co(1)–Co(3) edge which supports the bridging hydride is significantly longer (2.621 Å) than the Co(1)–Co(2) edge (2.557 Å), which is bridged by C(1), and the Co(2)–Co(3) edge (2.525 Å), which is bridged by N(1). While the projection of the hydride onto the tricobalt plane lies 0.19 Å within the tricobalt triangle, the ligand is better described as μ_2-H than μ_3-H since there are two short (1.41(5) and 1.65(5) Å) and one long (2.01(5) Å) Co–H distances. The Cp* ligands proximal to the bulky *tert*-butyl group of the formimidoyl ligand are displaced 0.68 and 0.64 Å out of the Co_3 plane and away from the formimidoyl ligand. In contrast, the centroid of the Cp* ligand bonded distal to the *tert*-butyl group is displaced out of the Co_3 plane by only 0.09 Å. The structure of the tricobalt core and bridging atoms of **4** is nearly identical with the core structures of the related imidoyl clusters $Os_3(CO)_9(\mu_2\text{-}H)(\mu_3\text{-}\eta^2\text{-}HC{=}NC_6H_5)$ (**6**),[17] $Fe_3(CO)_9(\mu_2\text{-}H)(\mu_3\text{-}\eta^2\text{-}CH_3C{=}NH)$ (**7**),[18] $[Re_3(\mu\text{-}H)_3(\mu_3\text{-}\eta^2\text{-}HC{=}NC_6H_{11})(CO)_9]^-$ (**8**),[19] and $Ru_3(CO)_9(\mu\text{-}H)(\mu_3\text{-}\eta^2\text{-}MeC{=}NEt)$ (**9**).[20]

The C(1)=N(1) distance (1.35 Å) of the formimidoyl ligand is longer than that of an uncomplexed C=N double bond (1.28 Å) and shorter than that of an uncomplexed C–N single bond (1.47 Å). This distance corresponds to a C–N bond order of about 1.5 and is consistent with the formimidoyl ligand bonding to the cluster face via σ-C, σ-N, and π-C=N interactions. The C(1)–N(1)–C(2) angle of 121° and the H(1a)–C(1)–N(1) angle of 122° suggest sp^2 hybridization of these metal-bound atoms. The C(1)=N(1) distance is similar to the C=N distances observed in other μ_3-η^2-imidoyl clusters, which range from 1.286 Å in **8** to 1.415 Å in **6**.

Observation of a Bis(isocyanide) Dihydride Cluster Intermediate prior to Formation of the Formimidoyl Cluster 4. Metal clusters of Ru,[21] Rh,[22] Os[23] and Ir[23,24] have been studied as potential homogeneous catalysts for the hydrogenation of CO, and evidence suggests that in some cases the active species is polynuclear. Formation of a metal formyl complex has been proposed as a key step in homogeneous CO reduction.[25] Unfortunately, the forcing conditions required to effect CO reduction preclude mechanistic study of the active catalyst.

Migrations to isocyanide ligands are more facile than migration to CO.[26] As a result, the insertion of isocyanides into metal–hydrogen bonds to produce formimidoyl complexes is commonly seen in both mononuclear[27]

(16) (a) Caddy, P.; Green, M.; O'Brien, E.; Smart, L. E.; Woodward, P. *Angew Chem., Int. Ed. Engl.* **1977**, *16*, 648. (b) Yamamoto, Y.; Mise, T.; Yamazaki, H. *Bull. Chem. Soc. Jpn.* **1978**, *51*, 2743. (c) Jones, W. D.; Feher, F. J. *Organometallics* **1983**, *2*, 686. (d) Belt, S. T.; Duckett, S. B.; Haddleton, D. M.; Perutz, R. N. *Organometallics* **1989**, *8*, 748. (e) Jones, W. D.; Duttweiler, R. P.; Feher, F. J. *Inorg. Chem.* **1990**, *29*, 1505. (f) Beaumont, I.; Wright, A. H. *J. Organomet. Chem.* **1992**, *425*, C11.

(17) (a) Adams, R. D.; Golembeski, N. M. *J. Am. Chem. Soc.* **1978**, *100*, 4622. (b) Adams, R. D.; Golembeski, N. M. *J. Am. Chem. Soc.* **1979**, *101*, 2579.

(18) Andrews, M. A.; van Buskirk, G.; Knobler, C. B.; Kaesz, H. D. *J. Am. Chem. Soc.* **1979**, *101*, 7245.

(19) (a) Beringhelli, T.; D'Alfonso, G.; Minoja, A.; Ciani, G.; Moret, M.; Sironi, A. *Organometallics* **1991**, *10*, 3131.

(20) Aime, S.; Gobetto, R.; Padovan, F.; Botta, M.; Rosenberg, E.; Gellert, R. W. *Organometallics* **1987**, *6*, 2074.

(21) (a) Dombek, B. D. *J. Am. Chem. Soc.* **1981**, *103*, 6508. (b) Knifton, J. F. *J. Am. Chem. Soc.* **1981**, *103*, 3959. (c) Knifton, J. F. *J. Catal.* **1982**, *76*, 101.

(22) Vidal, J. L.; Walker, W. E. *Inorg. Chem.* **1980**, *19*, 896.

(23) Thomas, M. G.; Beier, B. F.; Muetterties, E. L. *J. Am. Chem. Soc.* **1976**, *98*, 1296.

(24) Demitras, G. C.; Muetterties, E. L. *J. Am. Chem. Soc.* **1977**, *99*, 2796.

(25) Costa, L. C. *Catal. Rev.—Sci. Eng.* **1983**, *25*, 325.

(26) Singleton, E.; Oosthuizen, H. E. *Adv. Organomet. Chem.* **1983**, *22*, 209.

(27) (a) Facchin, G.; Uguagliati, P.; Michelin, R. A. *Organometallics* **1984**, *3*, 1818. (b) Christian, D. F.; Clark, G. R.; Roper, W. R.; Waters, J. M.; Whittle, K. R. *J. Chem. Soc., Chem. Commun.* **1972**, 458. (c) Clark, G. R.; Waters, J. M.; Whittle, K. R. *J. Chem. Soc., Dalton Trans.* **1975**, 2556. (d) Alcock, N. W.; Brown, J. M.; MacLean, T. D. *J. Chem. Soc., Chem. Commun.* **1984**, 1689. (e) Christian, D. F.; Clark, H. C. *J. Organomet. Chem.* **1975**, *85*, C9. (f) Christian, D. F.; Clark, H. C.; Stepaniak, R. F. *J. Organomet. Chem.* **1976**, *112*, 209. (g) Christian, D. F.; Roper, W. R. *J. Organomet. Chem.* **1974**, *80*, C35. (h) Wolczanski, P. T.; Bercaw, J. E. *J. Am. Chem. Soc.* **1979**, *101*, 6450.

Scheme 5

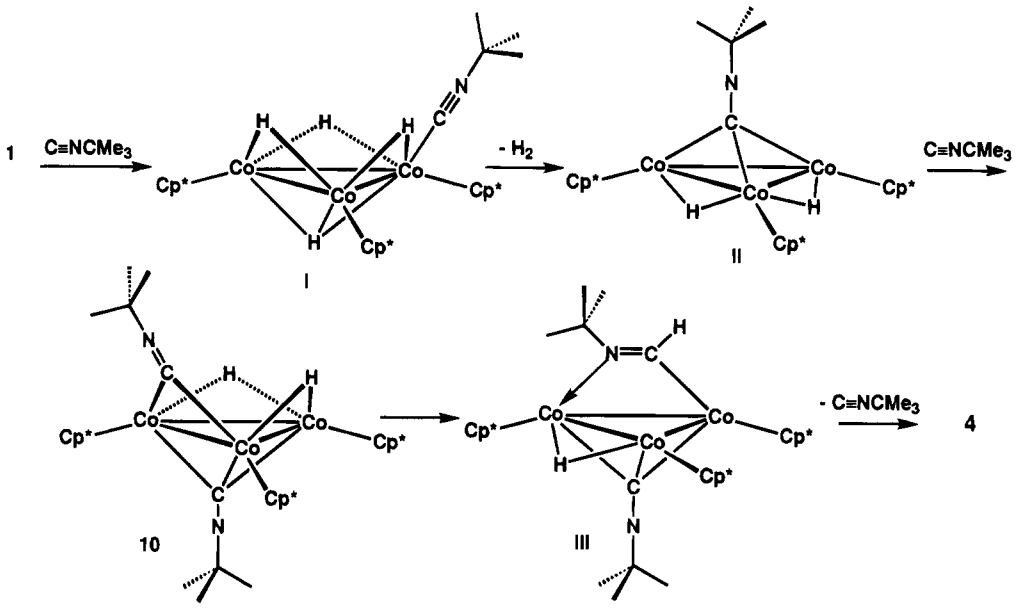

and dinuclear[28] systems but the insertion of CO into a metal–hydrogen bond to produce a formyl ligand has only rarely been observed.[29] In the case of clusters, isocyanide insertion into an M–H bond is of particular interest as a model for CO insertion in cluster-catalyzed CO reductions. Formimidoyl clusters of Re_3,[30] Fe_3,[31] Ru_3,[32] and Os_3[33] have been formed by the direct insertion of an isocyanide into an M–H bond, by intermolecular hydride attack on a coordinated isocyanide,[32] and from the unusual reaction of NMe_3 with $Os_3(CO)_{12}$.[33] Due to the importance of the unusually facile insertion of an isocyanide into an M–H bond which forms cluster **4**, we searched for intermediates in the reaction of **1** with *tert*-butyl isocyanide.

When a solution of **1** and excess C≡$NCMe_3$ in toluene-d_8 was warmed from −80 to −35 °C and monitored by ^{1}H NMR spectroscopy, a 2:1 ratio of two new Cp* signals at δ 1.95 and 1.59 began to appear after 15 min, along with the Cp* signal of **4** at δ 1.86. The relative intensity of the two signals reached a maximum of 35% after 2 h and then gradually decreased; the 2:1 ratio of the signals remained constant throughout. The Cp* resonances at δ 1.95 (30 H) and 1.59 (15 H) and signals at δ 1.13 (18 H) and −20.05 (2 H) are assigned to the 48-electron bis(isocyanide) dihydride cluster $Cp^*_3Co_3(\mu\text{-CNCMe}_3)_2(\mu\text{-H})_2$ (**10**). Although the structure of **10** rests solely on spectroscopic data, the proposed structure is isoelectronic with the dicarbonyl dihydride cluster **2**.

A plausible mechanism for the formation of intermediate **10** and its conversion to formimidoyl complex **4** is presented in Scheme 5. We suggest that coordination of isocyanide to the unsaturated tetrahydride cluster **1** forms the unobserved 48-electron intermediate $Cp^*_3Co_3(\mu\text{-H})_4(CNCMe_3)$ (**I**). Isolated clusters similar to **I** include $Os_3(CO)_{10}(\mu_2\text{-H})_2(CNC_6H_5)$, which forms the μ_2-formimidoyl complex $Os_3(CO)_{10}(\mu_2\text{-H})(\mu_2\text{-}\eta^2\text{-HC=NC}_6H_5)$ when heated to 80 °C,[17] and $Re_3(\mu\text{-H})_4(CO)_9(CNC_6H_{11})$, which reacts with PMe_2Ph to form the μ_2-formimidoyl complex $Re_3(\mu\text{-H})_3(CO)_9(\mu_2\text{-}\eta^2\text{-HC=NC}_6H_{11})(PMe_2Ph)$.[30] Next, we suggest that the 48-electron intermediate **I** loses H_2 to form the 46-electron mono(isocyanide) dihydride cluster **II**, which rapidly adds a second isocyanide to form the observed bis(isocyanide) dihydride cluster **10**. Conversion of **10** to **4** might then be completed by insertion of an isocyanide ligand into a Co–H bond of **10** to form the unobserved edge-bridged formimidoyl cluster $Cp^*_3Co_3(\mu\text{-CNCMe}_3)(\mu\text{-H})(\mu_2\text{-}\eta^2\text{-HC=NCMe}_3)$ (**III**) followed by expulsion of the isocyanide ligand to generate **4**.

Variable-Temperature ^{1}H NMR of 4. The X-ray crystal structure of **4** clearly indicated the presence of three inequivalent Cp* ligands. However, the room-temperature ^{1}H NMR spectrum of **4** displayed a single sharp Cp* resonance at δ 1.88. At −88 °C, a 1:2 ratio of Cp* resonances was observed at δ 1.94 and 1.81. As the temperature was increased, the Cp* resonance broadened and coalesced at −72 °C, forming a single resonance at −68 °C (Figure 4). In addition, the methyl groups of the *tert*-butyl unit became inequivalent at low temperature and split into a 2:1 ratio of methyl resonances at δ 1.51 and 1.44 at −88 °C. When the temperature was raised, these methyl resonances broadened and coalesced at −76 °C. Only a single formimidoyl resonance at δ 8.69 was seen over the entire temperature range from −88 to +25 °C.

The presence of a 2:1 ratio of Cp* resonances at −88 °C is consistent with the oscillation of a single terminus of the formimidoyl ligand between two cluster edges in concert with hydride migration in the opposite direction

(28) (a) Prest, D. W.; Mays, M. J.; Raithby, P. R. *J. Chem. Soc., Dalton Trans.* **1982**, 2021. (b) McKenna, S. T.; Anderson, R. A.; Muetterties, E. L. *Organometallics* **1986**, *5*, 2233. (c) Mays, M. J.; Prest, D. W.; Raithby, P. R. *J. Chem. Soc., Chem. Commun.* **1980**, 171. (d) Ciriano, M.; Green, M.; Gregson, D.; Howard, J. A. K.; Spencer, J. L.; Stone, F. G. A.; Woodward, P. *J. Chem. Soc., Dalton Trans.* **1979**, 1294. (e) Evans, W. J.; Meadows, J. H.; Hunter, W. E.; Atwood, J. L. *Organometallics* **1983**, *2*, 1252.

(29) (a) Fagan, P. J.; Moloy, K. G.; Marks, T. J. *J. Am. Chem. Soc.* **1981**, *103*, 6959. (b) Moloy, K. G.; Marks, T. J. *J. Am. Chem. Soc.* **1984**, *106*, 7051. (c) Wayland, B. B.; Woods, B. A. *J. Chem. Soc., Chem. Commun.* **1981**, 700.

(30) Beringhelli, T.; D'Alfonso, G.; Freni, M.; Ciani, G.; Moret, M.; Sironi, A. *J. Organomet. Chem.* **1990**, *399*, 291.

(31) (a) Bruce, M. I.; Hambley, T. W.; Nicholson, B. K. *J. Chem. Soc., Chem. Commun.* **1982**, 353. (b) Howell, J. A. S.; Mathur, P. *J. Chem. Soc., Chem. Commun.* **1981**, 263. (c) Howell, J. A. S.; Mathur, P. *J. Chem. Soc., Dalton Trans.* **1982**, 43. (d) Lentz, D.; Marschall, R. *Chem. Ber.* **1991**, *124*, 497.

(32) (a) Bruce, M. I.; Wallis, R. C. *J. Organomet. Chem.* **1979**, *164*, C6. (b) Bruce, M. I.; Wallis, R. C. *Aust. J. Chem.* **1982**, *35*, 709.

(33) Yin, C. C.; Deeming, A. J. *J. Organomet. Chem.* **1977**, *133*, 123.

Scheme 6

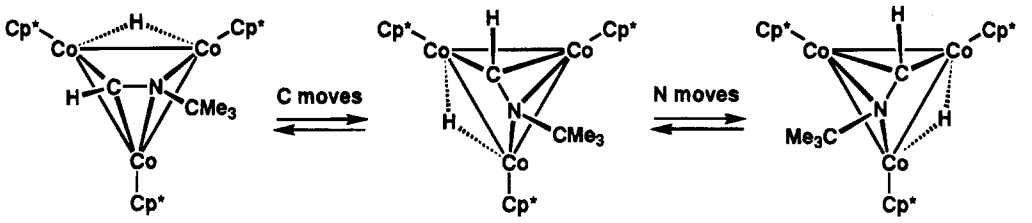

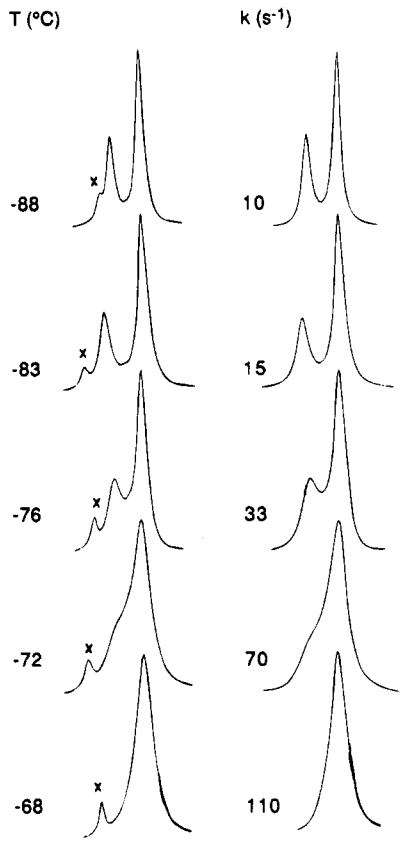

Figure 4. Variable temperature ^{1}H NMR spectra (500 MHz) of the Cp* region of **4** in toluene-d_8. Observed spectra and temperatures are on the left. Simulated spectra and rates are on the right. **x** denotes the $C_6D_5CHD_2$ resonance.

between the same two edges (Scheme 6). This oscillation creates a time-averaged plane of symmetry which contains one cobalt atom and bisects the opposite cluster edge. Edge to edge oscillation of either the carbon or the nitrogen bridge (but not both) equally well explains the 2:1 ratio of Cp* resonances. Because the Cp* ligands on the cobalt atoms bridged by nitrogen are both substantially displaced downward from the tricobalt plane and oscillation of the carbon terminus would require the least cluster rearrangement, we weakly favor carbon oscillation as the lower energy process. This is also consistent with the very rapid carbon migration (averaged Cp resonances at −100 °C) seen for $Cp_3Co_3(\mu_3\text{-}CO)(\mu_3\text{-}\eta^2\text{-}HC{\equiv}CCMe_3)$.[34] Rosenberg has suggested that nitrogen oscillation is faster than carbon oscillation in μ_3-η^2-imidoyl complexes.[35] The temperature-dependent NMR spectra of $Os_3(CO)_8(CNCMe_3)(\mu\text{-}H)(\mu_3\text{-}\eta^2\text{-}C{=}NCH_2CH_2CH_2)$ are consistent with more rapid nitrogen oscillation, assuming that the major species in solution corresponds to that seen for a related compound by X-ray crystallography.[35c] Other examples of "windshield wiper" fluctuation have been observed in clusters possessing μ_3-η^2-formimidoyl,[19,31b-d] imidoyl,[20,35] and alkynyl[36] ligands.

The coalescence of all three Cp* resonances above −72 °C is consistent with a second fluxional process in which both the carbon atom and the nitrogen atom of the formimidoyl ligand undergo edge to edge oscillation. The combination of edge to edge oscillation of both the carbon and nitrogen bridges creates a time-averaged 3-fold symmetry axis perpendicular to the Co_3 plane. Complete line-shape analysis of the Cp* resonances in the ^{1}H NMR spectrum of **4** in the temperature range from −88 to −68 °C established a barrier of $\Delta G^{\ddagger}_{200K}$ = 9.9(1) kcal mol^{-1} for complete rotation of the formimidoyl ligand about the tricobalt plane. This barrier is very similar to those observed in other formimidoyl and imidoyl clusters. For example, the barrier for rotation of the imidoyl ligand for cluster **8** was $\Delta G^{\ddagger}_{223K}$ = 9.8 kcal mol^{-1},[19] and the barrier for rotation of the formimidoyl ligand in cluster **9** was $\Delta G^{\ddagger}_{208K}$ = 10.0 kcal mol^{-1}.[20]

The unexpected observation of a 2:1 ratio of methyl resonances for the *tert*-butyl unit at −88 °C requires hindered rotation of the *tert*-butyl group. Two of the *tert*-butyl methyl groups are then averaged by the symmetry plane created by the oscillation of a single terminus of the formimidoyl ligand. Above −76 °C, the three *tert*-butyl methyl groups become equivalent, due to the 3-fold symmetry axis created by complete rotation of the formimidoyl ligand. Because the methyl resonances were broad, it was not possible to do a complete line-shape analysis to measure the barrier to exchange of methyl environments. However, the spectra were consistent with a barrier for methyl exchange similar to that for Cp* exchange. NMR inequivalent methyl resonances have been seen for the $SiMe_3$ groups in the closely related complex $Cp_3Co_3(\mu_3\text{-}\eta^2\text{-}Me_3SiC{\equiv}CSiMe_3)$[36a] and for *tert*-butyl groups in several compounds.[37]

(34) Barnes, C. E.; Orvis, J. A.; Finniss, G. M. *Organometallics* **1990**, *9*, 1695.

(35) (a) Rosenberg, E.; Kabir, S. E.; Hardcastle, K. I.; Day, M.; Wolf, E. *Organometallics* **1990**, *9*, 2214. (b) Day, M.; Espitia, D.; Hardcastle, K. I.; Kabir, S. E.; Rosenberg, E.; Gobetto, R.; Milone, L.; Osella, D. *Organometallics* **1991**, *10*, 3550. (c) Day, M.; Espitia, D.; Hardcastle, K. I.; Kabir, S. E.; McPhillips, T.; Rosenberg, E.; Gobetto, R.; Milone, L.; Osella, D. *Organometallics* **1993**, *12*, 2309.

(36) (a) Eaton, B.; O'Connor, J. M.; Vollhardt, K. P. C. *Organometallics* **1986**, *5*, 394. (b) Yamamoto, T.; Garber, A. R.; Bodner, G. M.; Todd, L. J.; Rausch, M. D.; Gardner, S. A. *J. Organomet. Chem.* **1973**, *56*, C23. (c) Todd, L. J.; Wilkinson, J. R.; Rausch, M. D.; Gardner, S. A.; Dickson, R. S. *J. Organomet. Chem.* **1975**, *101*, 133. (d) Deeming, A. J. *J. Organomet. Chem.* **1978**, *150*, 123. (e) Deeming, A. J.; Rothwell, I. P.; Hursthouse, M. B.; Backer-Dirks, J. D. J. *J. Chem. Soc., Dalton Trans.* **1981**, 1879. (f) Aime, S.; Gobetto, R.; Osella, D.; Milone, L.; Rosenberg, E. *Organometallics* **1982**, *1*, 640. (g) Aime, S.; Bertoncello, R.; Busetti, V.; Gobetto, R.; Granozzi, G.; Osella, D. *Inorg. Chem.* **1986**, *25*, 4004. (h) Rosenberg, E.; Bracker-Novak, J.; Gellert, R. W.; Aime, S.; Gobetto, R.; Osella, D. *J. Organomet. Chem.* **1989**, *365*, 163. (i) Manojlovic-Muir, L.; Muir, K. W.; Rashidi, M.; Schoettel, G.; Puddephatt, R. J. *Organometallics* **1991**, *10*, 1719.

(37) Sternhell, S. In *Dynamic Nuclear Magnetic Resonance Spectroscopy*; Jackman, L. M., Cotton, F. A., Eds.; Academic Press: New York, 1975; pp 163–201.

Scheme 7

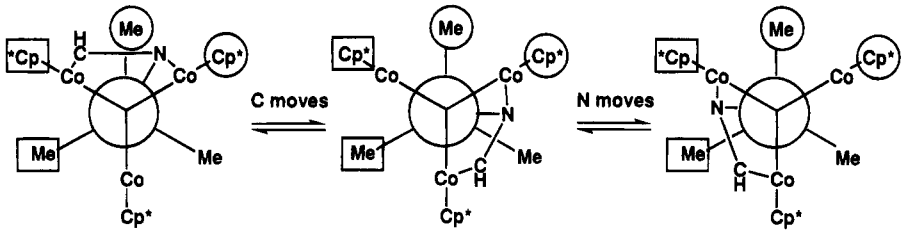

Scheme 8

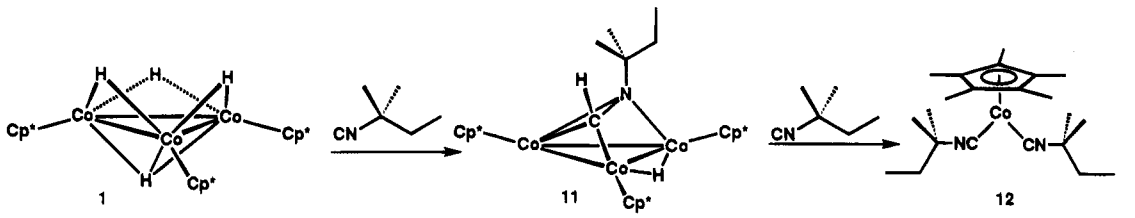

As illustrated in Scheme 7, the tricobalt formimidoyl cluster **4** can be thought of as having three layers of groups: a bottom layer of three methyl groups, a central layer containing the bridging formimidoyl ligand, and a top layer containing the Cp*Co units. It is important to note that even if there were no rotation of the *tert*-butyl group relative to the tricobalt triangle, the methyl and Cp* resonances would be equivalent at room temperature because of the formimidoyl rotation. To determine whether a tertiary alkyl group attached to nitrogen rotates relative to the tricobalt triangle, we synthesized $Cp^*_3Co_3(\mu_2\text{-}H)(\mu_3\text{-}\eta^2\text{-}CH{=}NCMe_2CH_2Me)$ (**11**), which possesses an N-alkyl group sterically similar to the *tert*-butyl group of **4** but which lacks 3-fold symmetry.

Reaction of 1 with *tert*-Amyl Isocyanide. The reaction of $Cp^*_3Co_3(\mu_2\text{-}H)_3(\mu_3\text{-}H)$ (**1**) and 3.5 equiv of *tert*-amyl isocyanide in benzene at room temperature for 12 h followed by evaporation of solvent produced an oily brown residue from which the bis(isocyanide) monomer $Cp^*Co(CNCMe_2CH_2Me)_2$ (**12**) was isolated in 28% yield by distillation and brown crystalline formimidoyl cluster $Cp^*_3Co_3(\mu_2\text{-}H)(\mu_3\text{-}\eta^2\text{-}CH{=}NCMe_2CH_2Me)$ (**11**) was obtained in 32% yield by crystallization from pentane (Scheme 8).

X-ray Crystal Structure of 11. The structure of **11** was determined by X-ray crystallography (Figure 5, Tables 1 and 4). Two crystallographically independent molecules, **11a** and **11b**, were present in the unit cell and differ only in the thermal parameters of the *N*-*tert*-amyl group. Molecule **11a** possesses less distortion and is shown in Figure 5. The $-CH_2Me$ moiety of the *N*-*tert*-amyl group is directed so that the C(2)–C(5) bond is perpendicular to the Co(1)–Co(3) bond axis. This location appears to be the least sterically crowded site, as the C(3) and C(4) *tert*-amyl methyl carbons are in closer contact with a Cp* methyl group than is the methylene carbon C(5). The closest through-space contacts for the carbon atoms β to the formimidoyl nitrogen atom and Cp* methyl groups are C(3)–C(23) = 3.540 Å, C(4)–C(33) = 3.443 Å, and C(5)–C(33) = 3.605 Å.

Variable-Temperature ^{1}H NMR of 11. The room-temperature ^{1}H NMR spectrum of **11** in toluene-d_8 displayed a single sharp resonance for the Cp* ligands at δ 1.87. At −87 °C a 1:1:1 ratio of Cp* resonances

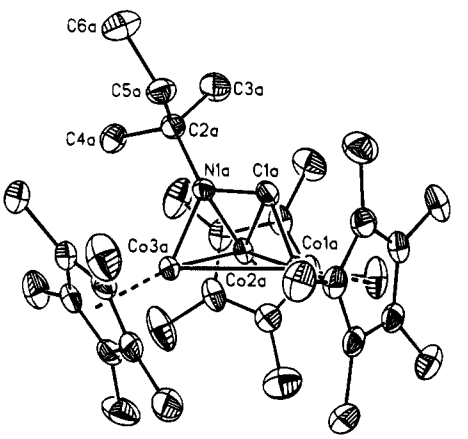

Figure 5. X-ray crystal structure of $Cp^*_3Co_3(\mu\text{-}H)(\mu_3\text{-}\eta^2\text{-}CH{=}NCMe_2CH_2Me)$ (**11a**) with thermal ellipsoids shown at the 35% probability level.

Table 4. Selected Bond Lengths (Å) and Angles (deg) for $Cp^*_3Co_3(\mu_2\text{-}H)(\mu_3\text{-}\eta^2\text{-}CH{=}NCMe_2CH_2Me)$ (11)

Co(1)–Co(2)	2.561(1)	Co(3)–N(1)	1.925(3)
Co(1)–Co(3)	2.623(1)	C(1)–N(1)	1.358(6)
Co(2)–Co(3)	2.540(1)	C(2)–N(1)	1.498(6)
Co(1)–C(1)	1.839(4)	Co(1)–Cp_{cent}	1.755
Co(2)–C(1)	1.966(5)	Co(2)–Cp_{cent}	1.755
Co(2)–N(1)	1.974(4)	Co(3)–Cp_{cent}	1.764
Co(1)–Co(2)–Co(3)	61.9(1)	C(1)–Co(2)–N(1)	40.3(2)
Co(1)–Co(3)–Co(2)	59.4(1)	Co(1)–C(1)–N(1)	116.0(3)
Co(2)–Co(1)–Co(3)	58.7(1)	Co(3)–N(1)–C(1)	103.4(3)
Co(1)–C(1)–Co(2)	84.5(2)	Co(2)–N(1)–C(2)	132.6(2)
Co(2)–N(1)–Co(3)	81.3(1)	Co(3)–N(1)–C(2)	130.5(3)
C(1)–N(1)–C(2)	120.7(3)		

was observed at δ 2.02, 1.91, and 1.86 (Figure 6). As the temperature was increased, the two outer resonances broadened and coalesced at about −64 °C, while the center resonance remained sharper and shifted slightly to lower frequency. At −56 °C, a partially resolved 2:1 ratio of resonances was observed at δ 1.91 and 1.88. As the temperature was increased further, the Cp* resonances coalesced at −50 °C and formed a single peak at −46 °C. Similarly, the two methyl groups of the *N*-*tert*-amyl moiety gave rise to a 1:1 ratio of resonances at δ 1.45 and 1.06 at −87 °C. As the temperature was increased, the peaks broadened over a wide temperature range and eventually formed a single resonance at δ 1.39 at −40 °C. At −87 °C, a

Scheme 9

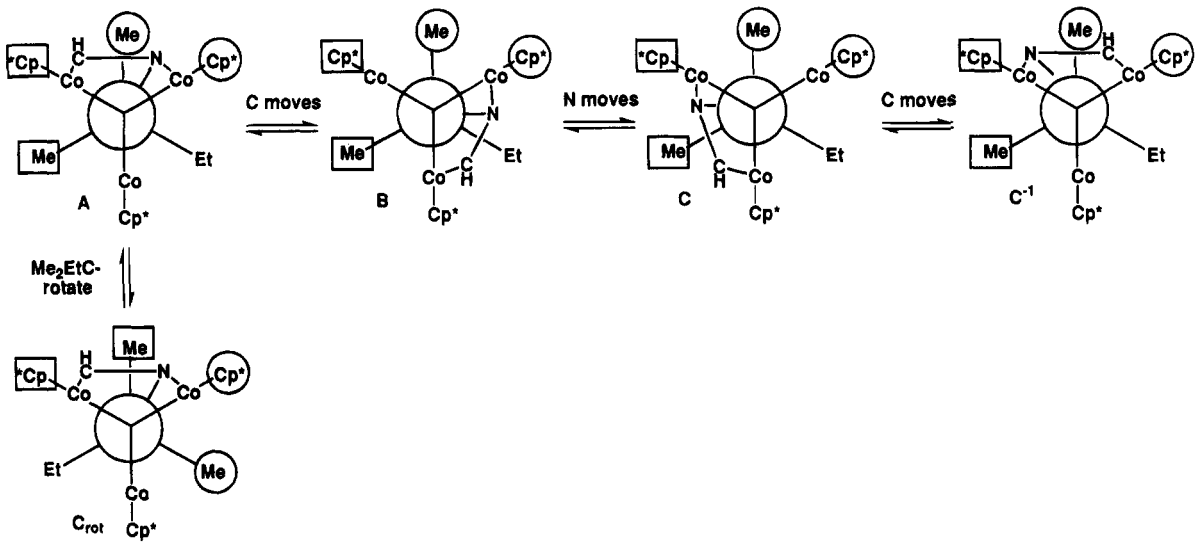

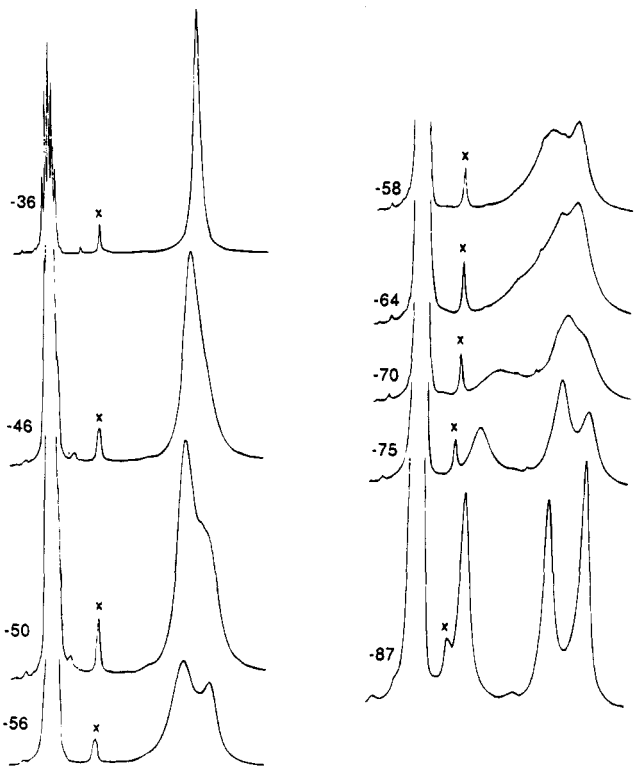

Figure 6. Variable-temperature ^{1}H NMR spectra of the Cp* region of **11** in toluene-d_8. Temperatures are given in °C; **x** denotes an impurity.

single resonance corresponding to the imidoyl hydrogen was observed at δ 8.50.

The spectrum of **11** at −87 °C, which shows three 1:1:1 Cp* resonances, two 1:1 methyl resonances for the *tert*-amyl group, and a single formimidoyl resonance, will be discussed first (Scheme 9). There are three possible rotameric diastereomers of **11** that differ in the relationship of the Et group and the formimidoyl ligand, which are shown as **A**, **B**, and **C**. For ease of discussion, we will assume that the rapid fluxional process involves carbon oscillation and that nitrogen oscillation is slower (similar conclusions would result if the relative rates were reversed). At −87 °C, fast carbon oscillation would rapidly interconvert **A** and **B** but their averaged spectra would still have three Cp* resonances, since both nitrogen oscillation and alkyl rotation are slow. Rapid carbon oscillation interconverts rotamer **C** with its enantiomer **C**$^{-1}$; this interchanges the environment of a pair of Cp* groups and a 2:1 ratio of Cp* resonances would be expected for **C**. The fact that only three out of the possible five Cp* resonances are seen and that only a single formimidoyl resonance is seen at −87 °C suggests that the solution may contain only a rapidly interconverting mixture of **A** and **B**. Conformation **B** was observed in the X-ray crystal structure of **11**.

When the temperature is raised from −87 to −56 °C, the three Cp* resonances are transformed into a 2:1 ratio of Cp* resonances. This is the spectrum expected if both carbon and nitrogen oscillation become fast (thereby interconverting **A**, **B**, and **C** and their enantiomers), but rotation of the CMe_2Et group relative to the $Cp^*_3Co_3$ triangle is slow. A barrier for the slower of the oscillation processes of $\Delta G^{\ddagger}$ = 9.9 kcal mol^{-1} was estimated from a peak separation of 80 Hz and a coalescence temperature of −64 °C. This barrier is the same as the 9.9 kcal mol^{-1} barrier observed for **4**.

When the temperature is raised further from −56 to −36 °C, the 2:1 Cp* resonances coalesce and then become a sharp singlet. This corresponds to rapid rotation of the CMe_2Et group relative to the $Cp^*_3Co_3$ triangle, which exchanges the environments of all three Cp* ligands. A barrier for alkyl rotation of $\Delta G^{\ddagger}$ = 10.5 kcal mol^{-1} was estimated from a peak separation of 50 Hz and a coalescence temperature of −50 °C. Thus, the barrier for tertiary alkyl rotation in this system is somewhat higher than the barrier for the slower of the carbon or nitrogen oscillation processes.

Experimental Section

General Methods. All manipulations were performed under a nitrogen atmosphere in an inert-atmosphere glovebox or by standard high-vacuum techniques. ^{1}H NMR spectra were obtained on a Bruker WP200, WP270, or AM500 spectrometer. ^{13}C NMR spectra were obtained on a Bruker AM500 (126 MHz) spectrometer. Probe temperatures were measured with a calibrated platinum resistance wire and are estimated to be accurate to ±1 °C. Line-shape analyses were performed using the program DNMR5.[38] Infrared spectra were recorded

(38) Stephenson, D. S.; Binsch, G. *Quantum Chemistry Program Exchange* **1978**, *10*, 365.

Table 5. Atomic Coordinates ($\times 10^4$) and Equivalent Isotropic Displacement Coefficients (Å $\times 10^3$) for $Cp^*_3Co_3(\mu_3\text{-}CO)(\mu_2\text{-}CO)(\mu\text{-}H)_2$ (2)

	x	y	z	U(eq)		x	y	z	U(eq)
Co(1)	2121(1)	5257(1)	2500	54(1)	C(4)	12(6)	3966(6)	2961(4)	74(3)
C(1)	3333	6667	3366(13)	114(7)	C(5)	2142(14)	2164(12)	2500	255(16)
O(1)	3333	6667	4149(8)	180(7)	C(6)	1064(12)	3101(12)	4163(7)	214(9)
C(2)	1348(10)	3023(9)	2500	98(6)	C(7)	−870(9)	4393(9)	3523(7)	173(7)
C(3)	848(8)	3371(7)	3230(5)	89(4)					

on a Mattson Polaris FT-IR spectrometer. Mass spectra were determined on a Kratos MS-80 spectrometer. Elemental analyses were performed by Desert Analytics (Tucson, AZ). Diethyl ether, hexane, pentane, and benzene were distilled from purple solutions of sodium and benzophenone. Benzene-d_6 and toluene-d_8 were distilled from sodium and benzophenone or from sodium/potassium alloy. *tert*-Butyl isocyanide (Fluka), CO (Airco), and ^{13}CO (Cambridge, 99% ^{13}C) were used as received. *tert*-Amyl isocyanide was prepared by the method of Gokel and Weber.[39] The temperature dependence of the solubility of hydrogen in benzene,[40] the density of benzene,[41] and the vapor pressure of benzene[41] were obtained from the literature.

$Cp^*_3Co_3(\mu_2\text{-}CO)(\mu_3\text{-}CO)(\mu_2\text{-}H)_2$ (2). A solution of $Cp^*_3Co_3(\mu_2\text{-}H)_3(\mu_3\text{-}H)$ (**1**; 26 mg, 0.044 mmol) in 3 mL of benzene was stirred overnight under CO (3.54 mL, 480 mmHg, 22 °C, 0.088 mmol) in a sealed 8 mL flask. Benzene was evaporated under vacuum, and the residue was crystallized from pentane at −20 °C to give **2** (17 mg, 61%) as black crystals. ^1H NMR (C_6D_6, 200 MHz): δ 1.63 (1 Cp*), 1.56 (2 Cp*), −32.26 (μ-H). IR (hexane): 1778, 1652 cm^{-1}. IR (KBr): 1770, 1650 cm^{-1}. HRMS (EI): calcd (found) for $C_{32}H_{45}O_2Co_3$ ($M^+ - 2H$) 638.1412 (638.1395). Anal. Calcd (found) for $C_{32}H_{47}O_2Co_3$: C, 60.04 (60.16); H, 7.40 (7.40).

$Cp^*_3Co_3(\mu_2\text{-}^{13}CO)(\mu_3\text{-}^{13}CO)(\mu\text{-}H)_2$ (2-($^{13}CO)_2$). A solution of **1** (3 mg, 0.005 mmol) in C_6D_6 (0.5 mL) in a resealable NMR tube was exposed to small amounts (<0.5 equiv) of ^{13}CO and monitored after each addition by ^1H NMR spectroscopy. Four additions of ^{13}CO provided **2-($^{13}CO)_2$**, which contained ~5% **1** by ^1H NMR analysis. ^1H NMR (C_6D_6, 200 MHz): δ 1.63 (1 Cp*), 1.56 (2 Cp*), −32.26 (t, J_{CH} = 9.2 Hz, μ-H). $^{13}C\{^1H\}$ NMR (C_6D_6, 126 MHz): δ 270.9, 97.7, 94.2, 11.1, 9.8.

Kinetics of the Conversion of 2 to 3. A resealable NMR tube containing **2** (3 mg, 0.005 mmol, 0.01 M), C_6D_6 (0.5 mL), and C_6Me_6 (1 mg, 0.01 M, internal standard) was heated to reflux under nitrogen (740 Torr, 80 °C). Temperature control was achieved by refluxing under a controlled pressure of N_2. The reaction was monitored periodically by ^1H NMR spectroscopy; the concentration of **2** was determined by integrating the Cp* resonances of **2** (δ 1.63 and 1.56) relative to the hexamethylbenzene resonance (δ 2.12). The first-order rate constant for the conversion of **2** to **3** was obtained from a plot of ln [**2**] versus time. First-order rate constants were obtained for reactions carried out in refluxing benzene at 71 °C (555 Torr) and 60 °C (390 Torr). The temperature dependence of the rate of conversion of **2** to **3** was obtained from a plot of ln k versus $1/T$ (K).

Equilibrium between 2 and 3 + H_2. A resealable 1.9 mL thick-walled NMR tube containing **2** (3 mg, 0.005 mmol, 0.009 M), C_6D_6 (0.5 mL), and C_6Me_6 (1 mg, 0.012 M) was sealed under 1 atm of H_2 at 77 K. The tube was heated to 83 °C and monitored periodically by ^1H NMR spectroscopy; concentrations of **2** and **3** were determined by integrating the Cp* resonances for **2** (δ 1.63 and 1.56) and **3** (δ 3.39) relative to the hexamethylbenzene resonance (δ 2.12). When no further change in the ratio **2**:**3** was detected (3 days), the tube was opened to a small-volume manometer (11.5 mL); the pressure increase indicated the presence of 0.27 mmol of H_2 (5.4 atm, 0.023 M at 83 °C) in the NMR tube. The concentration of H_2 in solution was calculated from tables of the temperature dependence of the solubility of hydrogen in benzene.[40]

$Cp^*_3Co_3(\mu_2\text{-}H)(\mu_3\text{-}\eta^2\text{-}CH{=}NCMe_3)$ (4). *tert*-Butyl isocyanide (41 μL, 30 mg, 0.36 mmol) and **1** (87 mg, 0.15 mmol) in 5 mL of benzene were stirred at room temperature for 12 h to form a brown solution. Benzene was evaporated under vacuum, and the residue was crystallized from pentane at −20 °C to give brown crystals of $Cp^*_3Co_3(\mu_2\text{-}H)(\mu_3\text{-}\eta^2\text{-}CH{=}NCMe_3)$ (**5**) (51 mg, 52%). ^1H NMR (toluene-d_8, 200 MHz): δ 8.69 (s, C*H*=N), 1.86 (C_5Me_5), 1.58 (s, $NCMe_3$) −20.42 (br s, Co−H). $^{13}C\{^1H\}$ NMR (toluene-d_8, 126 MHz): δ 155.2 (br, CH=N), 85.5 (C_5Me_5), 61.6 ($NCMe_3$), 31.2 ($NC\mathit{Me}_3$), 12.7 ($C_5\mathit{Me}_5$). HRMS (EI): calcd (found) for $C_{35}H_{55}NCo_3$ ($M^+ - H$) 666.2334, (666.2325). Anal. Calcd (found) for $C_{35}H_{56}NCo_3$: C, 62.97 (63.06); H, 8.45 (8.52).

$Cp^*Co(CNCMe_3)_2$ (5). *tert*-Butyl isocyanide (110 mg, 1.32 mmol) and **1** (57 mg, 0.10 mmol) in 3 mL of benzene were heated to 55 °C for 2.5 h to produce an orange solution. Benzene and unreacted $CNCMe_3$ were evaporated under vacuum, and the residue was chromatographed (SiO_2, Et_2O). The first orange band to elute was further purified by short-path vacuum distillation at 75 °C to give **5** (44 mg, 45%) as a viscous red oil. ^1H NMR (C_6D_6, 200 MHz): δ 2.00 (C_5Me_5), 1.17 ($CNCMe_3$). $^{13}C\{^1H\}$ NMR (126 MHz, C_6D_6): δ 190.5 (br, *C*NCMe$_3$), 92.0 (C_5Me_5), 55.7 ($NCMe_3$), 32.0 ($NC\mathit{Me}_3$), 11.3 ($C_5\mathit{Me}_5$). IR (hexane): 2096 (sh), 2005 (s), 1902 (s) cm^{-1}. HRMS (EI): calcd (found) for $C_{20}H_{33}N_2Co$ 360.1975 (360.1977). Because **5** is a viscous, air-sensitive oil, elemental analysis was not obtained. ^1H NMR data indicated that **5** was >98% pure.

^1H NMR Observation of $Cp^*_3Co_3(\mu\text{-}CNCMe_3)_2(\mu\text{-}H)_2$ (10). *tert*-Butyl isocyanide (10 μL, 90 μmol) was condensed at 77 K into a 5 mm NMR tube containing **1** (3 mg, 5 μmol) and toluene-d_8 (0.5 mL). The tube was sealed under vacuum, shaken at 195 K, and placed into the probe of a 500 MHz NMR spectrometer cooled to 195 K. The tube was warmed to 240 K for 1 h and then to 250 K for an additional 2 h. Signals assigned to **10** at δ 1.95 (30 H, C_5Me_5), 1.59 (15 H, C_5Me_5), 1.13 (18 H, $CNCMe_3$), and −20.05 (2 H, μ-H) were observed after 15 min at 240 K and reached a maximum relative intensity of 35% after 100 min.

$Cp^*_3Co_3(\mu_2\text{-}H)(\mu_3\text{-}\eta^2\text{-}CH{=}NCMe_2CH_2Me)$ (11) and $Cp^*Co(CNCMe_2CH_2Me)_2$ (12). *tert*-Amyl isocyanide (67 mg, 0.69 mmol) and **1** (110 mg, 0.18 mmol) in 8 mL of benzene were stirred at room temperature for 12 h to produce a brown solution. Filtration through Celite and evaporation of benzene under vacuum produced an oily solid. ^1H NMR analysis of the solid revealed Cp* resonances for **11** and **12** in a 1.2:1.0 ratio. Short-path vacuum distillation of the residue at 85 °C produced $Cp^*Co(CNCMe_2CH_2Me)_2$ (**12**; 61 mg, 28%) as a viscous orange oil. The distillation residue was extracted with pentane and filtered through Celite to yield $Cp^*_3Co_3(\mu\text{-}H)(\mu_3\text{-}\eta^2\text{-}CH{=}NCMe_2CH_2Me)$ (**11**; 40 mg, 32%) as a dark brown powder which was >95% pure by ^1H NMR. **11** was further purified by crystallization from pentane at −20 °C.

11: ^1H NMR (C_6D_6, 200 MHz) δ 8.74 (s, C*H*=N), 2.22 (q, J = 7.5 Hz, NCH_2Me), 1.87 (C_5Me_5), 1.38 (s, $NCMe_2$), 1.15 (t, J = 7.5 Hz, $NCH_2\mathit{Me}$), −20.55 (br s, Co−μ-H); $^{13}C\{^1H\}$ NMR (C_6D_6, 126 MHz) δ 155.8 (br, CH=N), 86.5 (C_5Me_5), 64.4 ($NCMe_2$), 37.6 (CH_2Me), 26.4 ($NC\mathit{Me}_2$), 12.7 ($C_5\mathit{Me}_5$), 10.8 ($CH_2\mathit{Me}$); HRMS (EI) calcd (found) for $C_{36}H_{57}NCo_3$ ($M^+ - H$)

(39) Gokel, G. W.; Widera, R. P.; Weber, W. P. *Org. Synth.* **1976**, *55*, 96.

(40) *Solubility Data Series: Hydrogen and Deuterium*; Young, C. L., Ed.; Pergamon Press: Oxford, U.K., 1981; Vol. 5/6, pp 159−167.

(41) *International Critical Tables of Numerical Data, Physics, Chemistry and Technology;* Washburn, E. W., Ed.; McGraw-Hill: London, 1928; Vol. III, pp 29, 39, 221.

Table 6. Atomic Coordinates ($\times 10^4$) and Equivalent Isotropic Displacement Coefficients (Å $\times 10^3$) for $Cp^*_3Co_3(\mu_2\text{-}H)(\mu_3\text{-}\eta^2\text{-}CH{=}NCMe_3)$ (4)

	x	y	z	$U(eq)^a$		x	y	z	$U(eq)^a$
Co(1)	1146(1)	1848(1)	1782(1)	12(1)	C(32)	−1290(5)	274(3)	1985(3)	14(2)
Co(2)	−1049(1)	1456(1)	2135(1)	12(1)	C(33)	−746(5)	427(3)	2750(3)	14(2)
Co(3)	−942(1)	2379(1)	1042(1)	13(1)	C(34)	−1631(5)	877(3)	3105(3)	14(2)
C(1)	121(5)	2312(3)	2429(3)	14(2)	C(35)	−2718(5)	1001(3)	2577(3)	16(2)
N(1)	−985(4)	2592(2)	2097(2)	12(1)	C(41)	−3486(5)	494(3)	1227(3)	28(2)
C(2)	−1681(5)	3222(3)	2471(3)	19(2)	C(42)	−670(5)	−216(3)	1432(3)	22(2)
C(3)	−3071(5)	3209(3)	2161(3)	24(2)	C(43)	415(5)	64(3)	3147(3)	25(2)
C(4)	−1017(6)	3973(3)	2264(3)	25(2)	C(44)	−1491(6)	1102(3)	3927(3)	28(2)
C(5)	−1577(5)	3136(3)	3331(3)	25(2)	C(45)	−3968(5)	1325(3)	2746(3)	28(2)
C(11)	2781(5)	1631(3)	2532(3)	16(2)	C(51)	−1610(5)	1985(3)	−49(3)	12(2)
C(12)	2815(5)	2381(3)	2205(3)	17(2)	C(52)	−499(5)	2443(3)	−80(3)	16(2)
C(13)	2851(5)	2299(3)	1411(3)	15(1)	C(53)	−747(5)	3196(3)	172(3)	16(2)
C(14)	2816(5)	1499(3)	1239(3)	14(1)	C(54)	−2054(5)	3208(3)	331(3)	19(2)
C(15)	2791(5)	1090(3)	1935(3)	13(2)	C(55)	−2579(5)	2460(3)	193(3)	16(2)
C(21)	2860(5)	1477(3)	3370(3)	23(2)	C(61)	−1728(5)	1167(3)	−325(3)	21(2)
C(22)	2934(5)	3126(3)	2633(3)	27(2)	C(62)	658(5)	2174(3)	−438(3)	24(2)
C(23)	3108(5)	2969(3)	903(3)	27(2)	C(63)	62(5)	3902(3)	137(3)	24(2)
C(24)	3012(5)	1112(3)	494(3)	22(2)	C(64)	−2806(6)	3940(3)	427(3)	30(2)
C(25)	2954(5)	225(3)	1998(3)	22(2)	C(65)	−3967(5)	2253(3)	201(3)	29(2)
C(31)	−2509(5)	617(3)	1882(3)	15(2)					

[a] Equivalent isotropic U, defined as one-third of the trace of the orthogonalized U_{ij} tensor.

Table 7. Atomic Coordinates ($\times 10^4$) and Equivalent Isotropic Displacement Coefficients (Å $\times 10^3$) for $Cp^*_3Co_3(\mu_2\text{-}H)(\mu_3\text{-}\eta^2\text{-}CH{=}NCMe_2CH_2Me)$ (11)

	x	y	z	$U(eq)$		x	y	z	$U(eq)$
Co(1A)	54(1)	7463(1)	9833(1)	33(1)	Co(1B)	2943(1)	1645(1)	4276(1)	33(1)
Co(2A)	2498(1)	7655(1)	10328(1)	35(1)	Co(2B)	4007(1)	2992(1)	5331(1)	47(1)
Co(3A)	1567(1)	6813(1)	8943(1)	34(1)	Co(3B)	1731(1)	2479(1)	5304(1)	34(1)
C(1A)	1322(4)	8237(2)	9873(2)	40(2)	C(1B)	3867(4)	1851(3)	5230(2)	43(2)
N(1A)	2180(3)	7961(2)	9445(2)	35(1)	N(1B)	3323(3)	2285(2)	5800(2)	44(1)
C(2A)	2948(4)	8524(3)	9216(3)	42(2)	C(2B)	3703(5)	2211(3)	6549(3)	61(2)
C(3A)	3394(5)	9361(3)	9862(3)	64(2)	C(3B)	5157(6)	2206(5)	6777(3)	94(3)
C(4A)	4120(4)	8157(3)	9001(3)	55(2)	C(4B)	3370(6)	2962(4)	7141(3)	83(3)
C(5A)	2031(4)	8625(3)	8554(3)	49(2)	C(5B)	2941(6)	1410(4)	6446(3)	74(3)
C(6A)	2674(6)	9108(4)	8170(3)	74(3)	C(6B)	3039(8)	1233(5)	7162(4)	117(5)
C(7A)	−1930(4)	7261(3)	9278(3)	46(2)	C(7B)	1854(4)	528(2)	3468(2)	41(2)
C(8A)	−1480(4)	8101(3)	9714(3)	45(2)	C(8B)	3078(4)	420(3)	3832(2)	42(2)
C(9A)	−1088(4)	8201(3)	10486(3)	46(2)	C(9B)	4044(4)	845(3)	3653(2)	44(2)
C(10A)	−1291(4)	7422(3)	10521(2)	43(2)	C(10B)	3436(5)	1221(3)	3177(2)	44(2)
C(11A)	−1793(4)	6843(3)	9781(2)	42(2)	C(11B)	2076(4)	1042(3)	3079(2)	41(2)
C(12A)	−2605(5)	6931(3)	8472(3)	62(2)	C(12B)	593(5)	54(3)	3407(3)	60(2)
C(13A)	−1513(5)	8771(3)	9422(3)	66(3)	C(13B)	3261(6)	−127(3)	4268(3)	63(2)
C(14A)	−670(5)	9020(3)	11127(3)	67(2)	C(14B)	5465(5)	822(3)	3875(3)	64(2)
C(15A)	−1214(5)	7242(3)	11221(3)	63(2)	C(15B)	4025(6)	1613(3)	2731(3)	66(2)
C(16A)	−2313(5)	5968(3)	9594(3)	66(3)	C(16B)	1102(5)	1214(3)	2520(3)	61(2)
C(17A)	2786(4)	7982(3)	11495(2)	49(2)	C(17B)	5462(5)	3421(3)	4923(3)	65(2)
C(18A)	3692(4)	8478(3)	11367(2)	49(2)	C(18B)	5962(5)	3542(4)	5665(4)	81(3)
C(19A)	4493(4)	7972(3)	10949(3)	54(2)	C(19B)	5252(6)	4066(4)	6112(4)	94(3)
C(20A)	4038(5)	7162(3)	10822(3)	56(2)	C(20B)	4294(6)	4263(3)	5651(5)	89(3)
C(21A)	2965(5)	7161(3)	11139(2)	50(2)	C(21B)	4385(6)	3852(3)	4892(4)	78(3)
C(22A)	1937(6)	8290(4)	12039(3)	77(3)	C(22B)	6099(7)	3026(4)	4303(4)	95(3)
C(23A)	3909(7)	9396(3)	11710(3)	81(3)	C(23B)	7189(7)	3253(6)	5962(5)	128(5)
C(24A)	5723(5)	8243(4)	10785(3)	85(3)	C(24B)	5590(8)	4459(5)	6960(4)	152(5)
C(25A)	4734(6)	6457(4)	10515(3)	94(3)	C(25B)	3473(7)	4897(3)	5927(6)	152(6)
C(26A)	2258(7)	6440(4)	11194(3)	86(3)	C(26B)	3601(7)	3941(5)	4224(6)	125(6)
C(27A)	2712(5)	5981(3)	8318(3)	48(2)	C(27B)	558(4)	3313(3)	5919(3)	47(2)
C(28A)	1999(5)	6322(3)	7841(2)	47(2)	C(28B)	260(4)	2524(3)	5944(3)	47(2)
C(29A)	679(5)	6131(3)	7795(2)	47(2)	C(29B)	−168(4)	1951(3)	5196(3)	43(2)
C(30A)	556(5)	5662(3)	8225(2)	46(2)	C(30B)	−168(4)	2375(3)	4708(2)	40(2)
C(31A)	1827(5)	5584(2)	8559(2)	47(2)	C(31B)	304(4)	3212(3)	5163(3)	41(2)
C(32A)	4137(5)	5976(3)	8454(3)	74(3)	C(32B)	871(5)	4092(3)	6584(3)	73(2)
C(33A)	2496(7)	6655(3)	7323(3)	76(3)	C(33B)	86(6)	2355(4)	6621(3)	77(3)
C(34A)	−390(6)	6269(4)	7255(3)	77(3)	C(34B)	−768(6)	1084(3)	4970(3)	73(3)
C(35A)	−664(6)	5206(3)	8242(3)	73(2)	C(35B)	−698(5)	2060(3)	3886(3)	64(2)
C(36A)	2104(7)	5043(3)	8993(3)	83(3)	C(36B)	266(6)	3868(3)	4863(3)	70(3)

680.2484 (680.2458). Anal. Calcd (found) for $C_{36}H_{58}NCo_3$: C, 63.43 (63.39); H, 8.58 (8.57).

12: ^1H NMR (C_6D_6, 200 MHz) δ 2.02 (C_5Me_5), 1.35 (q, J = 7.4 Hz, CH_2Me), 1.15 (s, NCMe_2), 0.96 (t, J = 7.4 Hz, CH_2Me); $^{13}C\{^1H\}$ NMR (126 MHz, C_6D_6) δ 188.2 (br, $CNCMe_2$), 91.8 (C_5Me_5), 59.0 ($NCMe_2$), 36.8 (CH_2Me), 29.8 (NCMe_2), 11.3 (C_5Me_5), 9.2 (CH_2Me); IR (hexane) 2124 (sh), 2014 (s), 1908 (s); HRMS (EI) calcd (found) for $C_{22}H_{37}N_2Co$ 388.2288 (388.2308). Because **12** is a viscous, air-sensitive oil, elemental analysis was not obtained. ^1H NMR data indicated that **12** was >95% pure.

X-ray Crystallographic Determinations and Refinements. Each crystal was coated in epoxy and mounted on the tip of a thin glass fiber. Diffraction data were obtained with graphite-monochromated Mo Kα radiation on either a Siemens P3f diffractometer at 108 K (**2**) or a Siemens P4RA diffractometer at 295 K (**4** and **11**) in the range $4 < 2\theta < 50°$

by the $\theta-2\theta$ scan technique. Automatic indexing of 18–20 well-centered reflections determined the unit cell; precise unit cell dimensions were determined by the least-squares refinement of well-centered, high-angle reflections ($25° < 2\theta < 30°$). Standard reflections for each data set showed no significant decrease in intensity throughout acquisition. Initial positions for Co atoms were found by direct methods, and all non-hydrogen atoms were located from successive difference Fourier maps. All non-hydrogen atoms were refined anisotropically; carbon-bound hydrogen atoms were fixed at idealized positions with isotropic thermal parameters of $U = 0.08$ Å^2. Crystallographic computations were performed employing SHELXTL-PLUS[42] software on VAX computers.

X-ray Crystallography of $Cp^*_3Co_3(\mu_3\text{-}CO)(\mu_2\text{-}CO)(\mu\text{-}H)_2$ (2). Slow cooling of a saturated pentane solution to −20 °C gave black crystals of **2** suitable for X-ray analysis. Systematic absences and statistical analyses of each data set were consistent with the space group $P6_3/m$. The 1587 reflections collected produced 602 independent, observed reflections ($|F| > 4.0\sigma(F)$). Crystallographic data (Table 1), atomic coordinates (Table 5), and selected bond lengths and selected bond angles (Table 2) are presented.

X-ray Crystallography of $Cp^*_3Co_3(\mu_2\text{-}H)(\mu_3\text{-}\eta^2\text{-}CH{=}NMe_3)$ (4). Slow cooling of a saturated pentane solution to −20 °C gave brown crystals of **4** suitable for X-ray analysis. Systematic absences uniquely defined the space group as $P2_1/n$. The 4013 reflections collected produced 3758 independent, observed reflections ($|F| > 4.0\sigma(F)$). Crystallographic data (Table 1), atomic coordinates (Table 6), and selected bond lengths and selected bond angles (Table 3) are presented.

X-ray Crystallography of $Cp^*_3Co_3(\mu_2\text{-}H)(\mu_3\text{-}\eta^2\text{-}CH{=}NMe_2CH_2Me)$ (11). Slow cooling of a saturated pentane solution to −20 °C gave purple crystals of **11** suitable for X-ray analysis. Cluster **11** crystallized in the triclinic space group $P\bar{1}$. The 11 265 reflections collected produced 8987 independent, observed reflections ($|F| > 4.0\sigma(F)$). Crystallographic data (Table 1), atomic coordinates (Table 7), and selected bond lengths and bond angles (Table 4) are presented.

Acknowledgment. Financial support from the Department of Energy, Office of Basic Energy Science, is gratefully acknowledged. Grants from the NSF (Grant No. CHE-9105497) and from the University of Wisconsin for the purchase of the X-ray instruments and computers are acknowledged. R.A.W. and S.L.H. thank the Department of Education for fellowships.

Supplementary Material Available: Tables of structure determination data, anisotropic thermal parameters for non-hydrogen atoms, selected interatomic distances and angles, and idealized atomic parameters for hydrogen atoms for compounds **2**, **4**, and **11** (33 pages). Ordering information is given on any current masthead page.

OM940462J

(42) SHELXTL-PLUS, Siemens Analytical X-Ray Instruments, Inc.